



ELSEVIER

Journal of Electroanalytical Chemistry 415 (1996) 165–167

JOURNAL OF  
ELECTROANALYTICAL  
CHEMISTRY

## Preliminary note

## Detection of CO desorbing from the Ni electrode surface by DEMS

C.F. Zinola<sup>a</sup>, E.J. Vasini<sup>b</sup>, U. Müller<sup>c</sup>, H. Baltruschat<sup>c,\*</sup>, A.J. Arvia<sup>b</sup><sup>a</sup> Facultad de Ciencias, Universidad de La República, Tristán Narvaja 1174, C.P. 1100, Montevideo, Uruguay<sup>b</sup> Instituto de Investigaciones Físicoquímicas Teóricas y Aplicadas-INIFTA, Facultad de Ciencias Exactas, Universidad Nacional de La Plata, Casilla de Correo 16, Suc. 4, 1900 La Plata, Argentina<sup>c</sup> Institute of Physical and Theoretical Chemistry, University of Bonn, Römerstr. 164, D-53117 Bonn, Germany

Received 28 April 1996; revised 3 May 1996

Keywords: Nickel; Carbon monoxide; DEMS

## 1. Introduction

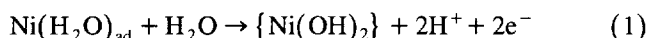
Electrochemical research on metal–CO interactions is generally related to the role of CO as a poison in the electro-oxidation reactions of organic fuels at noble metal electrodes. A small number of studies have treated the interaction of a nickel electrode with CO [1–3], either as a complement to studies of CO<sub>2</sub> electroreduction, in which case CO is considered as an intermediate [1], or in connection with an interest in Ni as a potential low cost electrocatalyst [2–4]. In addition, the study of adsorption and desorption reactions on nickel electrodes is also important for understanding the action of inhibitors. The adsorption of CO was also used to protect a Ni(111) surface during the transfer from UHV into alkaline electrolytes [5].

These studies show that CO is strongly adsorbed on the Ni electrode and that the nickel electrodisolution–nickel hydroxide precipitation voltammetric peak shifts to more positive potentials in the presence of CO. Thus it is concluded that the adsorbate inhibits the nickel electrodisolution process, allowing it to occur only after CO has been removed from the surface.

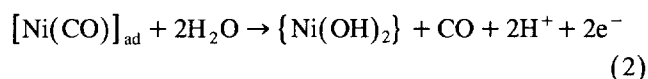
However, the mechanism of CO-adsorbate removal has not been determined experimentally, and two alternatives have been considered.

Hori and Murata [1], working at pH 6.8 in a HPO<sub>4</sub><sup>2-</sup>/H<sub>2</sub>PO<sub>4</sub><sup>-</sup> buffer electrolyte, proposed electro-oxidation of the protecting layer of adsorbed CO to CO<sub>2</sub>, followed by electro-oxidation of the Ni electrode. This was deduced from the values of the potential of the CO electro-oxidation on Pt and Rh electrodes and the standard equilibrium potential of the CO electro-oxidation reaction.

For solutions at pH values between 1 and 3 with H<sub>2</sub>SO<sub>4</sub> and HClO<sub>4</sub> electrolytes [2,3], it was proposed that CO removal consisted of the stripping of an adsorption layer that includes CO competitively adsorbed with water. This suggestion was based on the fact that the Ni oxidation peak in CO-containing acid solutions appeared only to be shifted in comparison with that in pure acid solutions [6]. The above mentioned potential shift has been shown to be consistent with the energy difference, estimated from gas-phase adsorption data [7,8], between the following reactions:



and



The present work uses on-line mass spectrometry (differential electrochemical mass spectrometry (DEMS)) to decide whether the anodic desorption product is really CO or rather CO<sub>2</sub>.

## 2. Experimental

The DEMS set-up, as well as the small volume flow cell used, have been described previously [9,10].

The Ni working electrode was prepared in the DEMS cell by Ni electrodeposition on a gold sputtered porous Teflon film with a geometric area of 0.5 cm<sup>2</sup>. The electrodeposition process was conducted at –0.4 V vs. RHE using a plating bath solution containing 300 g l<sup>-1</sup> NiSO<sub>4</sub> and H<sub>2</sub>SO<sub>4</sub> to obtain pH 3.5. After 15 min of deposition time, the cell was rinsed thoroughly with the corresponding working electrolyte solution.

\* Corresponding author.

The three working electrolytes used (0.5 and 0.005 M  $\text{H}_2\text{SO}_4$  and a 0.1 M  $\text{Na}_2\text{HPO}_4$  + 0.1 M  $\text{NaH}_2\text{PO}_4$  buffer), were prepared using Millipore-MilliQ<sup>®</sup> water and analytical grade reactives (p.a. Merck).

For 0.5 and 0.005 M  $\text{H}_2\text{SO}_4$  aqueous solutions an RHE was used, whereas for the phosphate buffer a  $\text{Hg}|\text{HgSO}_4|\text{Na}_2\text{SO}_4(\text{sat.})$  reference electrode, properly shielded in a double glass frit compartment, was employed. In all experiments a Pt wire was used as counter electrode.

Cyclic voltammograms were performed in Ar saturated working electrolyte solutions between  $-0.8$  and  $0.6$  V vs. RHE at  $10\text{ mV s}^{-1}$  until a stable profile was obtained (except for the 0.5 M  $\text{H}_2\text{SO}_4$  electrolyte for which only a preliminary cathodic sweep was performed owing to the high rate of Ni anodic dissolution in this strongly acidic solution). The solution was replaced with the corresponding CO saturated electrolyte under potential control at  $0.0$  V vs. RHE. After 5 min of adsorption time, CO was removed from the aqueous solution by electrolyte exchange and Ar bubbling, and anodic stripping voltammograms and on-line DEMS measurements were carried out at the same sweep rate, starting at the adsorption potential.

### 3. Results and discussion

The voltammetric and DEMS results exhibit the same general features in the three electrolyte solutions used. Fig. 1 shows the anodic voltammetric sweeps before and after CO adsorption (Fig. 1(a)) and the mass intensity–potential signals for  $m/z = 28$  (Fig. 1(b)) and  $m/z = 44$  (Fig. 1(c)) obtained in the CO desorption cycle for the 0.005 M  $\text{H}_2\text{SO}_4$  electrolyte. No other potential dependent mass signals were observed during the desorption scan and no potential dependent mass signals were observed in the cycle following the desorption scan.

The above mentioned anodic shift of the Ni electrodis-solution–precipitation peak in the presence of the CO adsorbate is clearly observed in Fig. 1(a). The corresponding voltammetric charge increases only slightly in the presence of the CO adsorbate, as already reported [1,2].

Fig. 1(b) and Fig. 1(c) show that the current intensity of the mass signal with  $m/z = 28$ , assigned to CO, is much larger than that of  $m/z = 44$ , assigned to  $\text{CO}_2$ . There is a contribution to  $m/z = 28$  from  $\text{CO}_2$  due to fragmentation (ca. 9% of the intensity of the  $m/z = 44$  peak), which is negligible in our case given the experimental relative intensities of both peaks. It must also be noted that the mass intensity signals are not parallel, the peak of the CO mass signal precedes the peak of the  $\text{CO}_2$  mass signal by ca. 80 mV and the  $\text{CO}_2$  mass signal starts to increase when the CO mass signal decays. It is also interesting to note that the maximum of the CO mass signal precedes the voltammetric peak by ca. 20 mV (i.e. 2 s). Such behaviour, i.e. non-oxidative anodic desorption, was also observed in

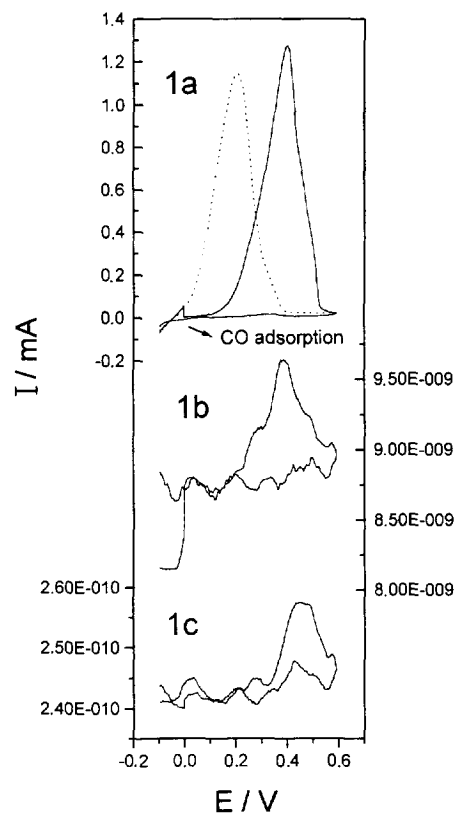


Fig. 1. Anodic voltammetric cycles before and after CO adsorption and potential dependent mass signals for the CO desorption cycle. Electrolyte, 0.005 M  $\text{H}_2\text{SO}_4$ ; working electrode, electrodeposited Ni on sputtered gold; reference electrode, RHE; counter electrode, Pt wire. (a) Anodic cycle before CO adsorption ( $\cdots$ ); CO adsorption followed by solution exchange and CO desorption cycle ( $\text{—}$ ) (see text). (b)  $m/z = 28$  ion current potential signal corresponding to the solid line cycle in (a). (The step at 0 V is due to an increase in the base signal of CO during adsorption of CO). (c)  $m/z = 44$  current–potential signal corresponding to the solid line cycle in (a).

the case of benzene adsorbed on Rh and Pd electrodes as opposed to Pt, on which benzene is completely oxidized to  $\text{CO}_2$  [11].

Table 1 shows the integrated mass intensity signals for all experimental conditions. It is immediately clear that the main mechanism for removal of the protective layer is CO stripping, about 10–20% of the adsorbed CO is oxidized to  $\text{CO}_2$ . The greatest proportion of  $\text{CO}_2$  occurs at neutral pH. It therefore may well be true that in alkaline solutions oxidation to  $\text{CO}_2$  predominates [5].

From the integrated mass intensity signals and the experimentally measured calibration constant ( $K^* = 5.5 \times 10^{-5}$ ) (cf. Ref. [9]) for the DEMS set-up, the absolute amount of adsorbed CO can be calculated to be 1.4, 6 and 12 nmol per square centimetre of geometric electrode surface for the phosphate, 5 mM  $\text{H}_2\text{SO}_4$  and 0.5 M  $\text{H}_2\text{SO}_4$  solutions respectively. The roughness factors of the electrodes used here are not known. Usually it is about 10 for sputtered Pt or Au electrodes. Owing to the electrodeposition of Ni, it is probably even higher in the present case. Comparing the above values with the amount of

Table 1  
Integrated charge under potential dependent mass signals ( $Q_{m/z=28}$  and  $Q_{m/z=44}$ ) observed in the anodic CO desorption scan for the experimental electrolytes

Electrolyte	$Q_{m/z=28} / 10^{-8} \text{ C}$	$Q_{m/z=44} / 10^{-8} \text{ C}$	$Q_{\text{el}} / \text{mC}$
0.1 M $\text{KH}_2\text{PO}_4$ + 0.1 M $\text{K}_2\text{HPO}_4$	0.29	0.083	1.4
0.005 M $\text{H}_2\text{SO}_4$	1.6	0.030	22
0.5 M $\text{H}_2\text{SO}_4$	3.1	0.23	603

surface Ni atoms (approximately  $2.6 \text{ nmol cm}^{-2}$  real area), it is clear that coverage with CO may be complete in the most acidic solution, but certainly not in the neutral solution. From the values given in Table 1 it can also be calculated that the relative contribution of reaction (2) to the overall current increases with increasing pH from 0.2 to 10%.

These experimental results suggest the following reaction sequence: (a) CO- and water- (or OH-containing species) are competitively adsorbed at the Ni|electrolyte interface; (b) Ni electrodisolution is inhibited by this strongly adsorbed CO; (c) an anodic stripping of the adsorbate, schematically represented by reaction (2), takes place at potentials which correspond to the rising part of the voltammetric peak; (d) this is followed by the oxidation of underlying Ni layers, thus, the CO mass current intensity signal reaches its maximum before the voltammetric peak, which is almost totally determined by the massive electrodisolution-precipitation process of nickel; (e) a small portion of the remaining adsorbate is oxidized to  $\text{CO}_2$ , probably induced by the co-adsorbed  $\text{OH}^-$  present at the Ni interface at this potential.

## Acknowledgements

The authors are indebted to Ingrid Vogel for the preparation of the gold sputtered films. C.F.Z. thanks the D.A.A.D. (Germany) and the Universidad de La República (Uruguay) for a scholarship granted. E.J.V. thanks the D.A.A.D. (Germany) and CONICET (Argentina) for a fellowship, and the C.I.C.Pcia.Bs.As. (Argentina) for financial support. H.B. thanks the Wissenschaftsministerium NRW for financial support through AGEF.

## References

- [1] Y. Hori and A. Murata, *Electrochim. Acta*, 35 (1990) 1777.
- [2] A.M. Castro Luna and A.J. Arvia, *J. Appl. Electrochem.*, 21 (1991) 435.
- [3] C.F. Zinola and A.M. Castro Luna, *Corros. Sci.*, 37 (1995) 1949.
- [4] C.F. Zinola, A.M. Castro Luna and A.J. Arvia, *J. Appl. Electrochem.*, 26 (1996) 325.
- [5] K. Wang, G.S. Chottiner and D.A. Scherson, *J. Phys. Chem.*, 97 (1993) 10108.
- [6] S.G. Real, J.R. Vilche and J.A. Arvia, *Corros. Sci.*, 20 (1980) 563.
- [7] D. Brennan and F.H. Hayes, *Philos. Trans. Roy. Soc. London*, A258 (1965) 347.
- [8] O.L.J. Gijman, M.M.J. van Zandvoort and F. Labohm, *J. Chem. Soc., Faraday Trans. 2*, 80 (1984) 771.
- [9] O. Wolter and J. Heitbaum, *Ber. Bunsenges. Phys. Chem.*, 88 (1984) 2.
- [10] N. Anastasijevic, G. Hambitzer, T. Hartung, J.-M. Zhu, H. Baltruschat and J. Heitbaum, *Dechema-Monographs*, 120 (1989) 255.
- [11] U. Schmiemann, Z. Jusys and H. Baltruschat, *Electrochim. Acta*, 39 (1994) 561.